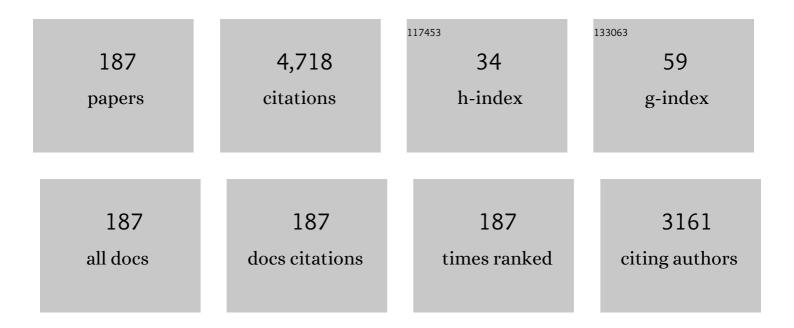
Ki Buem Kim

List of Publications by Year in descending order

Source: https://exaly.com/author-pdf/5353545/publications.pdf Version: 2024-02-01



KI RIIFM KIM

#	Article	IF	CITATIONS
1	"Work-Hardenable―Ductile Bulk Metallic Glass. Physical Review Letters, 2005, 94, 205501.	2.9	857
2	High strength ductile Cu-base metallic glass. Intermetallics, 2006, 14, 876-881.	1.8	123
3	Nanostructure–dendrite composites in the Fe–Zr binary alloy system exhibiting high strength and plasticity. Scripta Materialia, 2007, 57, 1153-1156.	2.6	105
4	High-strength bulk Al-based bimodal ultrafine eutectic composite with enhanced plasticity. Journal of Materials Research, 2009, 24, 2605-2609.	1.2	98
5	High strength ultrafine eutectic Fe–Nb–Al composites with enhanced plasticity. Intermetallics, 2008, 16, 642-650.	1.8	95
6	Microscopic deformation mechanism of a Ti66.1Nb13.9Ni4.8Cu8Sn7.2 nanostructure–dendrite composite. Acta Materialia, 2006, 54, 3701-3711.	3.8	93
7	Investigation of structure and mechanical properties of TiZrHfNiCuCo high entropy alloy thin films synthesized by magnetron sputtering. Journal of Alloys and Compounds, 2019, 797, 834-841.	2.8	84
8	Development of lightweight Mg Li Al alloys with high specific strength. Journal of Alloys and Compounds, 2016, 680, 116-120.	2.8	82
9	Interfacial reaction during the fabrication of Ni60Nb40 metallic glass particles-reinforced Al based MMCs. Materials Science & Engineering A: Structural Materials: Properties, Microstructure and Processing, 2007, 444, 206-213.	2.6	74
10	Amorphization in mechanically alloyed (Ti, Zr, Nb)–(Cu, Ni)–Al equiatomic alloys. Journal of Alloys and Compounds, 2007, 428, 157-163.	2.8	70
11	Deformation-induced rotational eutectic colonies containing length-scale heterogeneity in an ultrafine eutectic Fe83Ti7Zr6B4 alloy. Applied Physics Letters, 2007, 91, 131907.	1.5	69
12	Chemical evolution-induced strengthening on AlCoCrNi dual-phase high-entropy alloy with high specific strength. Journal of Alloys and Compounds, 2019, 777, 828-834.	2.8	64
13	Novel Multicomponent Amorphous Alloys. Materials Science Forum, 2002, 386-388, 27-32.	0.3	63
14	Propagation of shear bands and accommodation of shear strain in the Fe56Nb4Al40 ultrafine eutectic-dendrite composite. Applied Physics Letters, 2008, 92, .	1.5	63
15	Enhanced proton conductivity of yttrium-doped barium zirconate with sinterability in protonic ceramic fuel cells. Journal of Alloys and Compounds, 2015, 639, 435-444.	2.8	57
16	Influence of Zr content on phase formation, transition and mechanical behavior of Ni-Ti-Hf-Zr high temperature shape memory alloys. Journal of Alloys and Compounds, 2017, 692, 77-85.	2.8	52
17	Mechano-chemical synthesis and characterization of microstructure and magnetic properties of nanocrystalline Mn1â^'xZnxFe2O4. Journal of Alloys and Compounds, 2006, 424, 13-20.	2.8	49
18	Multi-phase Al-based ultrafine composite with multi-scale microstructure. Intermetallics, 2010, 18, 1829-1833.	1.8	48

#	Article	IF	CITATIONS
19	Study of Graphene-based 2D-Heterostructure Device Fabricated by All-Dry Transfer Process. ACS Applied Materials & Interfaces, 2016, 8, 3072-3078.	4.0	48
20	Metallic glass formation in multicomponent (Ti, Zr, Hf, Nb)–(Ni, Cu, Ag)–Al alloys. Journal of Non-Crystalline Solids, 2003, 317, 17-22.	1.5	47
21	Spectroscopic studies and electrical properties of transparent conductive films fabricated by using surfactant-stabilized single-walled carbon nanotube suspensions. Carbon, 2011, 49, 4301-4313.	5.4	47
22	Electrochemical properties of dual phase neodymium-doped ceria alkali carbonate composite electrolytes in intermediate temperature. Journal of Power Sources, 2015, 275, 563-572.	4.0	47
23	Degradation pattern prediction of a polymer electrolyte membrane fuel cell stack with series reliability structure via durability data of single cells. Applied Energy, 2014, 131, 48-55.	5.1	46
24	Micro-to-nano-scale deformation mechanisms of a bimodal ultrafine eutectic composite. Scientific Reports, 2014, 4, 6500.	1.6	46
25	Gradual martensitic transformation of B2 phase on TiCu-based bulk metallic glass composite during deformation. Intermetallics, 2016, 75, 1-7.	1.8	45
26	Understanding the relationship between microstructure and mechanical properties of Al–Cu–Si ultrafine eutectic composites. Materials and Design, 2016, 92, 1038-1045.	3.3	45
27	A study on the micro-evolution of mechanical property and microstructures in (Cu-30Fe)-2X alloys with the addition of minor alloying elements. Journal of Alloys and Compounds, 2019, 786, 341-345.	2.8	44
28	Effect of silicon on microstructure and mechanical properties of Cu-Fe alloys. Journal of Alloys and Compounds, 2017, 707, 184-188.	2.8	43
29	Bulk ultra-fine eutectic structure in Ti–Fe–base alloys. Journal of Alloys and Compounds, 2007, 434-435, 28-31.	2.8	42
30	Understanding microstructure and mechanical properties of (AlTa0.76) CoCrFeNi2.1 eutectic high entropy alloys via thermo-physical parameters. Journal of Materials Science and Technology, 2020, 57, 131-137.	5.6	42
31	Phase evolution, microstructure and mechanical properties of equi-atomic substituted TiZrHfNiCu and TiZrHfNiCuM (M = Co, Nb) high-entropy alloys. Metals and Materials International, 2016, 22, 551-556.	1.8	40
32	Outstanding strengthening behavior and dynamic mechanical properties of in-situ Al–Al3Ni composites by Cu addition. Composites Part B: Engineering, 2020, 189, 107891.	5.9	40
33	Work-hardening and plastic deformation behavior of Ti-based bulk metallic glass composites with bimodal sized B2 particles. Intermetallics, 2015, 62, 36-42.	1.8	38
34	High strength Ni–Zr binary ultrafine eutectic-dendrite composite with large plastic deformability. Applied Physics Letters, 2008, 93, .	1.5	36
35	Fe-based amorphous alloys as bipolar plates for PEM fuel cell. Journal of Power Sources, 2006, 159, 34-37.	4.0	35
36	Microstructure and mechanical properties of hierarchical multi-phase composites based on Al-Ni-type intermetallic compounds in the Al-Ni-Cu-Si alloy system. Journal of Alloys and Compounds, 2018, 749, 205-210.	2.8	35

#	Article	IF	CITATIONS
37	Modification of Oxygen-Ionic Transport Barrier of BaCo _{0.4} Zr _{0.1} Fe _{0.4} Y _{0.1} O _{3Â} Steam (Air) Electrode by Impregnating Samarium-Doped Ceria Nanoparticles for Proton-Conducting Reversible Solid Oxide Cells. Journal of the Electrochemical Society, 2019, 166, F746-F754.	1.3	35
38	Nano-scale structural evolution of quaternary AlCrFeNi based high entropy alloys by the addition of specific minor elements and its effect on mechanical characteristics. Journal of Alloys and Compounds, 2021, 868, 159217.	2.8	34
39	Ti-base bulk nanostructure-dendrite composites: Microstructure and deformation. Materials Science & Engineering A: Structural Materials: Properties, Microstructure and Processing, 2007, 449-451, 24-29.	2.6	33
40	Propagation of shear bands in a Cu47.5Zr47.5Al5 bulk metallic glass. Journal of Materials Research, 2008, 23, 6-12.	1.2	32
41	Heterogeneous eutectic structure in Ti–Fe–Sn alloys. Intermetallics, 2011, 19, 536-540.	1.8	30
42	Formation of ductile ultrafine eutectic structure in Ti–Fe–Sn alloy. Materials Science & Engineering A: Structural Materials: Properties, Microstructure and Processing, 2007, 449-451, 737-740.	2.6	29
43	Flexible polymer dispersed liquid crystal film with graphene transparent electrodes. Current Applied Physics, 2016, 16, 409-414.	1.1	29
44	Medium range ordering and its effect on plasticity of Fe–Mn–B–Y–Nb bulk metallic glass. Philosophical Magazine, 2010, 90, 2619-2633.	0.7	28
45	Crystallization, high temperature deformation behavior and solid-to-solid formability of a Ti-based bulk metallic glass within supercooled liquid region. Journal of Alloys and Compounds, 2016, 663, 270-278.	2.8	28
46	Microstructural investigation of a deformed Ti66.1Cu8Ni4.8Sn7.2Nb13.9 nanostructure–dendrite composite. Journal of Alloys and Compounds, 2007, 434-435, 106-109.	2.8	27
47	Phase transformations in mechanically milled and annealed single-phase β-Al3Mg2. Acta Materialia, 2008, 56, 1136-1143.	3.8	27
48	Combinatorial Influence of Bimodal Size of B2 TiCu Compounds on Plasticity of Ti-Cu-Ni-Zr-Sn-Si Bulk Metallic Glass Composites. Metallurgical and Materials Transactions A: Physical Metallurgy and Materials Science, 2014, 45, 2376-2381.	1.1	27
49	Tailoring the corrosion behavior of Fe-based metallic glasses through inducing Nb-triggered netlike structure. Corrosion Science, 2019, 147, 94-107.	3.0	27
50	Plastic deformation behavior of Fe–Co–B–Si–Nb–Cr bulk metallic glasses under nanoindentation. Journal of Alloys and Compounds, 2014, 587, 415-419.	2.8	26
51	Degradation analysis of anode-supported intermediate temperature-solid oxide fuel cells under various failure modes. Journal of Power Sources, 2015, 276, 120-132.	4.0	26
52	Influence of silicon content on microstructure and mechanical properties of Ti-Cr-Si alloys. Journal of Alloys and Compounds, 2018, 737, 53-57.	2.8	26
53	Influence of heterogeneities with different length scale on the plasticity of Fe-base ultrafine eutectic alloys. Journal of Materials Research, 2008, 23, 2003-2008.	1.2	25
54	Improving the plasticity and strength of Fe–Nb–B ultrafine eutectic composite. Materials & Design, 2015, 76, 190-195.	5.1	25

#	Article	IF	CITATIONS
55	Effect of boron addition on thermal and mechanical properties of Co-Cr-Mo-C-(B) glass-forming alloys. Intermetallics, 2018, 99, 1-7.	1.8	25
56	Investigation of phase-transformation path in TiZrHf(VNbTa)x refractory high-entropy alloys and its effect on mechanical property. Journal of Alloys and Compounds, 2021, 886, 161187.	2.8	25
57	Formation of Metallic Glasses in Novel (Ti ₃₃ Zr ₃₃ Hf ₃₃) _{100-x-y} (Ni ₅₀ Cu <sub Alloys. Materials Transactions, 2003, 44, 411-413.</sub 	s>50< ¢64 IB>) <s⊵48>x</s⊵48>
58	Enhancement of plasticity in Ti-rich Ti–Zr–Be–Cu–Ni–Ta bulk glassy alloy via introducing the structural inhomogeneity. Journal of Materials Research, 2008, 23, 2984-2989.	1.2	24
59	Influence of microstructural evolution on mechanical behavior of Fe–Nb–B ultrafine composites with a correlation to elastic modulus and hardness. Journal of Alloys and Compounds, 2015, 647, 886-891.	2.8	24
60	Favorable microstructural modulation and enhancement of mechanical properties of Ti–Fe–Nb ultrafine composites. Philosophical Magazine Letters, 2009, 89, 623-632.	0.5	23
61	Chemical heterogeneity-induced plasticity in Ti–Fe–Bi ultrafine eutectic alloys. Materials & Design, 2014, 60, 363-367.	5.1	23
62	High-current field emission of point-type carbon nanotube emitters on Ni-coated metal wires. Carbon, 2012, 50, 2126-2133.	5.4	22
63	Low-cost beta titanium cast alloys with good tensile properties developed with addition of commercial material. Journal of Alloys and Compounds, 2019, 793, 271-276.	2.8	22
64	New para-magnetic (CoFeNi)50(CrMo)50-(CB) (x = 20, 25, 30) non-equiatomic high entropy metallic glasses with wide supercooled liquid region and excellent mechanical properties. Journal of Materials Science and Technology, 2020, 43, 135-143.	5.6	22
65	Cooperative deformation behavior between the shear band and boundary sliding of an Al-based nanostructure-dendrite composite. Materials Science & Engineering A: Structural Materials: Properties, Microstructure and Processing, 2018, 735, 81-88.	2.6	21
66	Understanding the microstructure and mechanical properties of Ta Al0.7CoCrFeNi2.1 eutectic high entropy composites: Multi-scale deformation mechanism analysis. Composites Part B: Engineering, 2021, 214, 108750.	5.9	21
67	Beyond strength-ductility trade-off: 3D interconnected heterostructured composites by liquid metal dealloying. Composites Part B: Engineering, 2021, 225, 109266.	5.9	21
68	Crystallization Behavior and Microhardness Evolution in Al92â^'xNi8Lax Amorphous Alloys. Journal of Materials Research, 2005, 20, 2927-2933.	1.2	20
69	Crack evolution in bulk metallic glasses. Journal of Applied Physics, 2009, 106, .	1.1	20
70	Structural and Mechanical Properties of AlCoCrNi High Entropy Nitride Films: Influence of Process Pressure. Coatings, 2020, 10, 10.	1.2	20
71	Sn effect on microstructure and mechanical properties of ultrafine eutectic Ti–Fe–Sn alloys. Journal of Alloys and Compounds, 2009, 483, 44-46.	2.8	19
72	Effect of Ca addition on the plastic deformation behavior of extruded Mg-11Li-3Al-1Sn-0.4Mn alloy. Journal of Alloys and Compounds, 2016, 687, 821-826.	2.8	19

Кі Вием Кім

#	Article	IF	CITATIONS
73	Microstructure and mechanical properties of the as-cast and warm rolled Mg-9Li-x(Al-Si)-yTi alloys with xÂ=Â1, 3, 5 and yÂ=Â0.05Âwt.%. Journal of Alloys and Compounds, 2017, 711, 243-249.	2.8	19
74	Fabrication of a bulk icosahedral material through mechanical alloying of the powder mixture Ti41.5Zr41.5Ni17. Materials Letters, 2002, 52, 75-79.	1.3	18
75	Formation of icosahedral phase in an Al93Fe3Cr2Ti2 bulk alloy. Journal of Alloys and Compounds, 2007, 436, L1-L4.	2.8	18
76	Martensitic transformation in a B2-containing CuZr-based BMG composite revealed by in situ neutron diffraction. Journal of Alloys and Compounds, 2017, 723, 714-721.	2.8	18
77	Mechanical properties and microstructural change in (Cu–Fe) immiscible metal matrix composite: Effect of Mg on secondary phase separation. Journal of Materials Research and Technology, 2020, 9, 15989-15995.	2.6	18
78	Mechanical properties of large-scale Mg–Cu–Zn ultrafine eutectic composites. Journal of Alloys and Compounds, 2009, 481, 135-139.	2.8	17
79	Evolution of constitution, structure, and mechanical properties in Fe–Ti–Zr–B heterogeneous multiphase composites. Journal of Materials Research, 2011, 26, 365-371.	1.2	17
80	Characterization and deformation behavior of Ti hybrid compacts with solid-to-porous gradient structure. Materials & Design, 2014, 60, 66-71.	5.1	17
81	High strength porous Ti–6Al–4V foams synthesized by solid state powder processing. Journal Physics D: Applied Physics, 2008, 41, 105404.	1.3	16
82	Influence of spherical particles and interfacial stress distribution on viscous flow behavior of Ti uâ€Niâ€Zrâ€6n bulk metallic glass composites. Intermetallics, 2017, 91, 90-94.	1.8	16
83	Grain refinement to improve thermoelectric and mechanical performance in n-type Bi2Te2.7Se0.3 alloys. Materials Chemistry and Physics, 2020, 256, 123699.	2.0	16
84	Designing of Fe-containing (Ti33Zr33Hf33)-(Ni50Cu50) high entropy alloys developed by equiatomic substitution: phase evolution and mechanical properties. Journal of Materials Research and Technology, 2020, 9, 7732-7739.	2.6	16
85	Consolidation of mechanical alloyed Ti–37.5at.% Si powder mixture using an electro-discharge technique. Materials Science & Engineering A: Structural Materials: Properties, Microstructure and Processing, 2007, 467, 89-92.	2.6	14
86	Role of heterogeneity on deformation behavior of bulk metallic glasses. Journal of Alloys and Compounds, 2009, 486, 233-236.	2.8	14
87	Microstructural Modulations Enhance the Mechanical Properties in Al–Cu–(Si, Ga) Ultrafine Composites. Advanced Engineering Materials, 2010, 12, 1137-1141.	1.6	14
88	Influence and mitigation methods of reaction intermediates on cell performance in direct methanol fuel cell system. Journal of Power Sources, 2011, 196, 5446-5452.	4.0	14
89	Post-mortem analysis of a long-term tested proton exchange membrane fuel cell stack under low cathode humidification conditions. Journal of Power Sources, 2014, 253, 90-97.	4.0	14
90	Relationship between phase stability and mechanical properties on near/metastable β-type Ti–Cr-(Mn) cast alloys. Journal of Alloys and Compounds, 2020, 821, 153516.	2.8	14

#	Article	IF	CITATIONS
91	Hydrogen-induced amorphization and embrittlement resistance in Ti-based in situ composite with bcc-phase in an amorphous matrix. Journal of Materials Research, 2007, 22, 428-436.	1.2	13
92	Formation of porous metallic glass compacts by electro-discharge sintering. Journal of Alloys and Compounds, 2011, 509, S184-S187.	2.8	13
93	Optimization of mechanical properties of Ti–Fe–Sn alloys by controlling heterogeneous eutectic structure. Intermetallics, 2012, 23, 27-31.	1.8	13
94	Heterogeneous duplex structured Ti–Sn–Mo alloys with high strength and large plastic deformability. Journal of Alloys and Compounds, 2013, 574, 546-551.	2.8	13
95	Development of coherent-precipitate-hardened high-entropy alloys with hierarchical NiAl/Ni2TiAl precipitates in CrMnFeCoNiAlxTiy alloys. Materials Science & Engineering A: Structural Materials: Properties, Microstructure and Processing, 2021, 823, 141763.	2.6	13
96	Microstructural evolution and mechanical properties of Mg–Cu–Zn ultrafine eutectic composites. Journal of Materials Research, 2009, 24, 2892-2898.	1.2	12
97	Solid-state phase transformation-induced heterogeneous duplex structure in Ti–Sn–Fe alloys. Journal of Alloys and Compounds, 2012, 515, 86-89.	2.8	12
98	Crystallization and phase transformation behavior of TiCu-based bulk metallic glass composite with B2 particles. Journal of Alloys and Compounds, 2017, 707, 87-91.	2.8	12
99	Structure modification and recovery of amorphous Fe73.5Si13.5B9Nb3Cu1 magnetic ribbons after autoclave treatment: SAXS and thermodynamic analysis. Journal of Materials Science and Technology, 2019, 35, 118-126.	5.6	12
100	Studies on directly grown few layer graphene processed using tape-peeling method. Carbon, 2020, 158, 749-755.	5.4	12
101	Structural relaxation and glass transition behavior of novel (Ti33Zr33Hf33)50(Ni50Cu50)40Al10 alloy developed by equiatomic substitution. Journal of Non-Crystalline Solids, 2007, 353, 3338-3341.	1.5	11
102	Formation of bimodal eutectic structure in Ti63.5Fe30.5Sn6 and Mg72Cu5Zn23 alloys. Journal of Alloys and Compounds, 2011, 509, S353-S356.	2.8	11
103	Necking mechanisms on porous metallic glass and W compacts using electro-discharge sintering. Journal of Alloys and Compounds, 2012, 536, S78-S82.	2.8	11
104	Influence of Nb on microstructure and mechanical properties of Ti-Sn ultrafine eutectic alloy. Metals and Materials International, 2017, 23, 20-25.	1.8	11
105	Development of High Strength Ni–Cu–Zr–Ti–Si–Sn In-Situ Bulk Metallic Glass Composites Reinforced by Hard B2 Phase. Metals and Materials International, 2018, 24, 241-247.	1.8	11
106	Compositional tuning-induced permanent color adjustment and mechanical properties: Binary Cu-Mg colored metallic system. Materials and Design, 2019, 175, 107814.	3.3	11
107	Investigation on the Relationship Between Transition Energy and the Color Change of Cu–M Alloys. Metals and Materials International, 2019, 25, 539-545.	1.8	11
108	Toughening mechanisms of a Ti-based nanostructured composite containing ductile dendrites. International Journal of Materials Research, 2005, 96, 675-680.	0.8	11

Кі Вием Кім

#	Article	IF	CITATIONS
109	Nanocrystalline single-phase high-entropy alloy synthesized by using intermetallic compound type (TiZrHf)-(NiCuCo) high-entropy metallic glass precursor. Scripta Materialia, 2022, 209, 114391.	2.6	11
110	Enhancing Corrosion and Wear Resistance of AA6061 by Friction Stir Processing with Fe78Si9B13 Glass Particles. Materials, 2015, 8, 5084-5097.	1.3	10
111	Design of nano-scale multilayered nitride hard coatings deposited by arc ion plating process: Microstructural and mechanical characterization. Journal of Materials Research and Technology, 2021, 15, 572-581.	2.6	10
112	Novel Multicomponent Amorphous Alloys. Journal of Metastable and Nanocrystalline Materials, 2002, 13, 27-32.	0.1	9
113	Novel Multicomponent Alloys. Journal of Metastable and Nanocrystalline Materials, 2005, 24-25, 1-6.	0.1	9
114	Effect of cooling rate on microstructure and glass-forming ability of a (Ti33Zr33Hf33)70(Ni50Cu50)20Al10 alloy. Intermetallics, 2006, 14, 972-977.	1.8	9
115	Enhanced thermal stability of the devitrified nanoscale icosahedral phase in novel multicomponent amorphous alloys. Journal of Materials Research, 2006, 21, 823-831.	1.2	9
116	Devitrification of nano-scale icosahedral phase in multicomponent alloys. Materials Science & Engineering A: Structural Materials: Properties, Microstructure and Processing, 2007, 449-451, 983-986.	2.6	9
117	Mechanical behavior of metallic glass reinforced nanostructured tungsten composites synthesized by spark plasma sintering. Intermetallics, 2010, 18, 2009-2013.	1.8	9
118	Microstructural modulation of Ti–Fe–V ultrafine eutectic alloys with enhanced mechanical properties. Journal of Alloys and Compounds, 2010, 491, 178-181.	2.8	9
119	Field emission characteristics of carbon nanotube films fabricated on a metal mesh by filtration. Journal of Alloys and Compounds, 2012, 521, 126-133.	2.8	9
120	Thermally-triggered Dual In-situ Self-healing Metallic Materials. Scientific Reports, 2018, 8, 2120.	1.6	9
121	Development of Precipitation-Strengthened Al0.8NbTiVM (M = Co, Ni) Light-Weight Refractory High-Entropy Alloys. Materials, 2021, 14, 2085.	1.3	9
122	Stress-induced transformation behavior in near-eutectic (AlNi2)70-Co30Cr medium entropy alloys. Journal of Alloys and Compounds, 2022, 891, 161995.	2.8	9
123	Effect of solubility on strengthening of Ag–Cu ultrafine eutectic composites. Journal of Alloys and Compounds, 2011, 509, 9015-9018.	2.8	8
124	Developing high-strength ferritic alloys reinforced by combination of hierarchical and laves precipitates. Journal of Alloys and Compounds, 2021, 856, 158162.	2.8	8
125	Ozone Electrical Trimming of Carbon Nanotubes to Improve Their Field-Emission Lifetime and Uniformity. Journal of the Korean Physical Society, 2009, 54, 185-189.	0.3	8
126	Hierarchical heterostructured FeCr–(Mg–Mg2Ni) composite with 3D interconnected and lamellar structures synthesized by liquid metal dealloying. Journal of Materials Research and Technology, 2021, 15, 4573-4579.	2.6	8

#	Article	IF	CITATIONS
127	Effect of Cu on local amorphization in bulk Ni–Ti–Zr–Si alloys during solidification. Acta Materialia, 2006, 54, 3141-3150.	3.8	7
128	Microstructural comparison of Zr73.5Nb9Cu7Ni1Al9.5 nanostructure-dendrite composites produced by different casting techniques. Materials Science & Engineering A: Structural Materials: Properties, Microstructure and Processing, 2007, 449-451, 747-751.	2.6	7
129	Microstructure and mechanical properties of metallic glass/metallic glass composites. Journal of Alloys and Compounds, 2009, 483, 286-288.	2.8	7
130	Stable operation of air-blowing direct methanol fuel cell stacks through uniform oxidant supply by varying fluid flow fixtures and developing the flow sensor. International Journal of Hydrogen Energy, 2011, 36, 9205-9215.	3.8	7
131	Role of tri-capped triangular prism (TTP) polyhedra in formation and destabilization of Fe–Y–B glassy alloys. Journal of Non-Crystalline Solids, 2015, 425, 67-73.	1.5	7
132	Influence of N2 Gas Flow Ratio and Working Pressure on Amorphous Mo–Si–N Coating during Magnetron Sputtering. Coatings, 2020, 10, 34.	1.2	7
133	Development of coloring alloys: Color design for lightweight Al-Mg-Si alloys. Materials and Design, 2021, 200, 109449.	3.3	7
134	Formation of in-situ nanoscale Ag particles in (Ti0.33Zr0.33Hf0.33)40(Ni0.33Cu0.33Ag0.33)50Al10 alloy with wide supercooled liquid region. Materials Letters, 2005, 59, 1117-1120.	1.3	6
135	Metallic glass formation in the Cu47Ti33Zr11Ni8Si1 alloy. Materials Science & Engineering A: Structural Materials: Properties, Microstructure and Processing, 2007, 444, 257-264.	2.6	6
136	Synthesis of bulk amorphous composites with three amorphous phases by consolidation of milled amorphous powders. Intermetallics, 2010, 18, 2019-2023.	1.8	6
137	High-speed atomic force microscopy with phase-detection. Current Applied Physics, 2012, 12, 989-994.	1.1	6
138	Thermal analysis of directional pressure annealed Fe 78 Si 9 B 13 amorphous ribbons. Thermochimica Acta, 2018, 661, 67-77.	1.2	6
139	Co-Cr-Mo-C-B metallic glasses with wide supercooled liquid region obtained by systematic adjustment of the metalloid ratio. Journal of Non-Crystalline Solids, 2019, 505, 310-319.	1.5	6
140	Phase Transformation and Work-hardening Behavior of Ti-based Bulk Metallic Glass Composite. Applied Microscopy, 2015, 45, 37-43.	0.8	6
141	Structural evolution of the Ti70Ni15Al15 powders prepared by mechanical alloying. Materials Science & Engineering A: Structural Materials: Properties, Microstructure and Processing, 2001, 300, 148-152.	2.6	5
142	Glass Forming Ability and Crystallization Behaviour of New Multicomponent (Ti ₃₃ Zr ₃₃ Hf ₃₃) ₆₀ (Ni ₅₀ Cu ₅₀)< Alloy Developed by Equiatomic Substitution. Journal of Metastable and Nanocrystalline Materials, 2003, 15-16, 143-148.	sub>200.1	ıb>Al ₂₀
143	Formation of reactive layers in brazed Ti and Cu using a melt-spun Zr41.2Ti13.8Ni10.0Cu12.5Be22.5 alloy. Materials Letters, 2008, 62, 4483-4485.	1.3	5
144	Formation of deformation-induced bimodal grain structure of a high strength Ti ₉₃ Co ₇ alloy with enhancing plasticity. Journal Physics D: Applied Physics, 2009, 42, 032002.	1.3	5

9

Кі Вием Кім

#	Article	IF	CITATIONS
145	Effect of micro and nanoparticle inorganic fillers on the field emission characteristics of photosensitive carbon nanotube pastes. Applied Surface Science, 2010, 256, 2636-2642.	3.1	5
146	FABRICATION OF POROUS Ti- AND W-COMPACTS BY ELECTRO-DISCHARGE-SINTERING PROCESS. Surface Review and Letters, 2010, 17, 245-250.	0.5	5
147	Effect of martensitic ω phase on mechanical properties of Ti100â^'xCox alloys with x=5, 7 and 9. Intermetallics, 2010, 18, 725-729.	1.8	5
148	Microstructure and mechanical properties of Fe–Si–Ti–(Cu, Al) heterostructured ultrafine composites. Journal of Alloys and Compounds, 2011, 509, S367-S370.	2.8	5
149	Mechanically stable tuning fork sensor with high quality factor for the atomic force microscope. Scanning, 2014, 36, 632-639.	0.7	5
150	Designing porous metallic glass compact enclosed with surface iron oxides. Journal of Alloys and Compounds, 2015, 635, 233-237.	2.8	5
151	Effect of Metallic Glass Particle Size on the Contact Resistance of Ag/Metallic Glass Electrode. Metallurgical and Materials Transactions A: Physical Metallurgy and Materials Science, 2015, 46, 2443-2448.	1.1	5
152	Investigation of graphene dispersion on thermoelectric, magnetic, and mechanical properties of p-type Bi0.5Sb1.5Te3 alloys. Materials Chemistry and Physics, 2021, 266, 124512.	2.0	5
153	Formation of inhomogeneous micro-scale pores attributed ultralow Ϊlat and concurrent enhancement of thermoelectric performance in p-type Bi0.5Sb1.5Te3 alloys. Journal of Alloys and Compounds, 2021, 881, 160499.	2.8	5
154	Thermal Stability, Mechanical Properties and Magnetic Properties of Fe-based Amorphous Ribbons with the Addition of Mo and Nb. Journal of Magnetics, 2013, 18, 395-399.	0.2	5
155	Crystallization Behaviour of Novel(Ti ₃₃ Zr ₃₃ Hf ₃₃) _{100-x} (Ni ₅₀ Cu _{50 Alloys with X=48 to 55. Journal of Metastable and Nanocrystalline Materials, 2005, 24-25, 657-660.}	ˈ/subo≽j)≺su	b>xk/sub>
156	Effects of Co on the microstructures and mechanical properties of Ti ₅₀ Cu ₅₀ _{â^`} <i>_x</i> Co <i>_x</i> alloys (<i>x</i> = 0–25 at.%). Philosophical Magazine Letters, 2010, 90, 43-50.	0.5	4
157	Effect of Si on microstructure and mechanical properties of Fe-based ultrafine eutectic composites. Intermetallics, 2010, 18, 1856-1859.	1.8	4
158	Mechanical, deformation and fracture behaviors of bulk metallic glass composites reinforced by spherical B2 particles. Progress in Natural Science: Materials International, 2018, 28, 704-710.	1.8	4
159	Crystallization Kinetics and Thermo-Mechanical Behavior on Supercooled Liquid Region of Ti–Cu–Ni–Zr–Sn–Si Bulk Metallic Glass. Science of Advanced Materials, 2016, 8, 1989-1994.	0.1	4
160	Formation of nanocrystals in Ti78Fe15Si7 amorphous alloy with a wide supercooled liquid region. Materials Science & Engineering A: Structural Materials: Properties, Microstructure and Processing, 2004, 366, 421-425.	2.6	3
161	Influence of additional elements on the development of nanoscale heterogeneities in (TiCu)-based bulk metallic glasses with enhanced ductility. Journal of Materials Research, 2007, 22, 2223-2229.	1.2	3
162	Formation of nano-scale ï‰-phase in arc-melted micron-scale dendrite reinforced Zr73.5Nb9Cu7Ni1Al9.5 ultrafine composite during heat treatment. Intermetallics, 2008, 16, 538-543.	1.8	3

#	Article	IF	CITATIONS
163	Carbide formation in electric-discharge-sintered Ti3Al compact caused by steric acid in ball-milled Ti and Al powder mixture. Ceramics International, 2018, 44, 19771-19778.	2.3	3
164	Ultrafine shape memory alloys synthesized using a metastable metallic glass precursor with polymorphic crystallization. Applied Materials Today, 2021, 22, 100961.	2.3	3
165	Cryo-Casting for Controlled Decomposition of Cu–Zr–Al Bulk Metallic Glass into Nanomaterials: Implications for Design Optimization. ACS Applied Nano Materials, 2021, 4, 7771-7780.	2.4	3
166	Synthesis of High Strength Bulk Nanocrystalline Alloys Containing Remaining Amorphous Phase. Journal of Metastable and Nanocrystalline Materials, 1999, 1, 1-8.	0.1	2
167	Devitrification of nano-scale icosahedral phase in (Ti0.33Zr0.33Hf0.33)50(Ni0.5Cu0.5)40Al10 alloy with enlarging supercooled liquid region. Materials Letters, 2005, 59, 1771-1774.	1.3	2
168	Ti oxynitriding of microporous Ti–6Al–4V compact by electrodischarge sintering in an N2 atmosphere. Scripta Materialia, 2007, 57, 129-132.	2.6	2
169	Real-time atomic force microscopy in lubrication condition. Ultramicroscopy, 2010, 110, 826-830.	0.8	2
170	Influence of hetero-duplex structure on mechanical properties of Mg–Al/Cu–Zn alloys. Materials Science & Engineering A: Structural Materials: Properties, Microstructure and Processing, 2010, 528, 371-378.	2.6	2
171	Deformation mechanisms of a bimodal eutectic Mg72Cu5Zn23 ultrafine composite. Materials Letters, 2010, 64, 534-536.	1.3	2
172	Decomposition of icosahedral phase in Ti52Zr28Ni20 powder during electro-discharge sintering. Journal of Alloys and Compounds, 2010, 504, S302-S305.	2.8	2
173	Effect of Nb on microstructure and mechanical properties of ultrafine eutectic Fe–Ni–B–Si composites. Journal of Alloys and Compounds, 2010, 504, S487-S490.	2.8	2
174	Enhancement of mechanical properties in a Fe81Nb9B10 ultrafine-eutectic composite with in-situ polygonal pro-eutectic and encapsulating eutectic structure. Journal of Alloys and Compounds, 2015, 643, S204-S208.	2.8	2
175	Influence of directional microstructure on mechanical properties in Alâ€based ultrafine bimodal lamellar structured alloy. Material Design and Processing Communications, 2019, 1, e52.	0.5	2
176	Encapsulation of a gradient Al2O3 layer on hierarchical structured substrate via two-step hybrid processes. Materials and Design, 2019, 167, 107616.	3.3	2
177	Formation of photo-reactive heterostructure from a multicomponent amorphous alloy with atomically random distribution. Journal of Materials Science and Technology, 2022, 109, 245-253.	5.6	2
178	Fabrication of ultrafine powder using processing control agent, and investigation of its effect on microstructure and thermoelectric properties of p-type (Bi, Sb)2Te3 alloys. Advanced Powder Technology, 2022, 33, 103386.	2.0	2
179	Development and Characterization of Blue-Colored Mg2Si-Based Recycled Alloys Using Scrap Light Metals. Journal of Sustainable Metallurgy, 2022, 8, 673-683.	1.1	2
180	Deformation and fracture of Ti-base nanostructured composite. International Journal of Materials Research, 2008, 99, 985-990.	0.1	1

#	Article	IF	CITATIONS
101	MICROSTRUCTURAL EVOLUTION AND MECHANICAL PROERTIES OF Ti -(Ni ,) Tj ETQq1	1 0.78431	L4 rgBT /Ove
181	Physics B, 2009, 23, 953-959.	1.0	T
182	DEVELOPMENT OF HIGH STRENGTH Mg - Cu - Zn ULTRAFINE EUTECTIC COMPOSITES WITH ENHANCED PLASTICITY. International Journal of Modern Physics B, 2009, 23, 947-952.	1.0	1
183	TiCu-Based Bulk Metallic Glasses Exhibiting Large Compressive Plastic Strain . Applied Mechanics and Materials, 2011, 138-139, 624-629.	0.2	1
184	Evolution on Microstructure and Mechanical Property of Ti65Fe35 Hypereutectic Alloys by Adding Low Melting Temperature Elements. Korean Journal of Materials Research, 2017, 27, 557-562.	0.1	1
185	TEM INVESTIGATION ON CRYSTALLIZATION BEHAVIOR OF A Fe ₆₈ C _{10.5} Si _{4.4} BBULK METALLIC GLASS. International Journal of Modern Physics B, 2009, 23, 1223-1228.	> ւ.ո ւե>6.5	dsub> <fon< td=""></fon<>
186	Experimental data of inorganic gel based smart window using silica sol–gel process. Data in Brief, 2016, 9, 716-722.	0.5	0
187	Influence of Minor Element on Microstructure and Mechanical Properties of TiFe Ultrafine Eutectic Alloys, Korean Journal of Materials Research, 2012, 22, 615-619,	0.1	0